

# Visualization of Diffusion Tensor Data using Evenly Spaced Streamlines

Dorit Merhof<sup>1,2</sup>, Markus Sonntag<sup>2</sup>, Frank Enders<sup>1,2</sup>, Peter Hastreiter<sup>1,2</sup>,  
Rudolf Fahlbusch<sup>1</sup>, Christopher Nimsky<sup>1</sup>, Günther Greiner<sup>2</sup>

<sup>1</sup>Neurocenter, Dept. of Neurosurgery

Schwabachanlage 6, 91054 Erlangen, Germany

<sup>2</sup> Computer Graphics Group, University of Erlangen-Nuremberg  
Am Weichselgarten 9, 91058 Erlangen, Germany

## Abstract

Diffusion tensor imaging allows investigating white matter structures in vivo which is of particular interest for neurosurgery. A promising approach for the reconstruction of neural pathways are streamline based techniques commonly referred to as fiber tracking. However, due to the diverging nature of tract systems, the density of streamlines varies over the domain without control resulting in sparse areas as well as cramped regions. To overcome this problem, we adapted the concept of evenly spaced streamlines to fiber tracking providing streamlines equally distributed over the domain. Additionally, we incorporated evenly spaced streamlines into region of interest based tracking. We also investigated an adaptive control of the distance between separate streamlines depending on the magnitude of anisotropic diffusion which provides a mechanism to emphasize dominant tract systems.

## 1 Introduction

Diffusion tensor imaging (DTI) has shown potential in providing information about the location of white matter tracts within the human brain. In white matter the diffusion of water molecules is anisotropic due to the long cylindrical shape of myelinated nerve fibers. Contrarily, in areas of grey matter the diffusion probability is equally distributed since rather round shaped grey matter cells dominate. DTI thus allows reconstructing white matter structures to study neural anatomy of the human brain.

The directional variation of diffusion has to be measured for at least six non-collinear gradient directions. These directional diffusion images serve as a basis for the computation of diffusion tensors.

The resulting second order tensors characterize the diffusion probabilities within tissue. To exploit the contained information the eigensystem of each tensor is evaluated. Thereby, the eigenvector corresponding to the largest eigenvalue, in the following referred to as major eigenvector, indicates the direction of highest diffusion which correlates with the course of white matter fibers.

Tracking algorithms, which are based on streamline techniques known from flow visualization, utilize the major eigenvector to compute streamlines representing white matter anatomy. They often utilize thresholds, angle criterions, regularization techniques [1] and local filters [2] to improve tracking results. Due to their effectiveness, these techniques for the visualization of DTI data are subject of ongoing research [3, 4, 5, 6, 7].

Considering medical application, streamline tracking is currently one of the preferred techniques for planning in neurosurgery [8, 9]. It offers support to avoid postoperative neurological deficits by providing information about the location of white matter structures in vivo.

In spite of the benefits of streamline visualizations, they also have some drawbacks. In general, spatial resolution techniques such as streamlines suffer from a limited spatial resolution which constrain their significance. In regions containing only a limited number of streamlines, features of the data may remain concealed. Similarly, the effectiveness of the streamline methods critically depends on the placement of the initial seed points. To overcome these problems, evenly spaced streamlines for effective user-controlled streamline placement have been presented in the literature [10, 11]. The benefits of this approach were adapted to fiber tracking [7] to obtain uniformly distributed stream-

lines. This is of special interest for fibers of the corona radiata which ascend through the brain stem and diverge as they reach the cortex. The distribution of generic streamlines becomes sparser as they approach upper regions of the brain providing only rare information about the location of white matter. Adapting evenly spaced streamlines in the context of fiber tracking allows better capturing of the features contained within the data.

In this work an efficient 3D implementation of evenly spaced streamlines for fiber tracking is presented comprising data structures for fast access, a decider for streamline termination as well as a scheme for placement of new seed points in 3D. Furthermore, we extended the approach to enable region of interest (ROI) based tracking as well. We also added an adaptive control of the separating distance between evenly spaced streamlines which depends on the magnitude of diffusion. In this way, additional content within the data is visualized by making dominant tract systems perceptually more apparent and providing visual enhancement.

## 2 Method

In this section, the algorithm for evenly spaced streamlines in the context of fiber tracking is described. An introduction to DTI data and fiber tracking is given in Section 2.1 and 2.2. General features of the algorithm are outlined in Section 2.3. A perceptual enhancement, where the density of streamlines is controlled by the degree of diffusion, is presented in Section 2.4. Special features for extracting separate tract systems using ROIs are covered in Section 2.5.

### 2.1 Diffusion tensor data

DTI is an imaging technique which is capable to measure the diffusion properties of water molecules within tissue. Diffusion images are acquired for at least six different gradient directions. Additionally, a reference image without gradient direction is measured. These datasets enable to compute a diffusion tensor for each voxel. An efficient way for computing diffusion tensors is outlined in [12]. Each resulting diffusion tensor  $\mathbf{D}$

$$\mathbf{D} = \begin{pmatrix} D_{xx} & D_{xy} & D_{xz} \\ D_{xy} & D_{yy} & D_{yz} \\ D_{xz} & D_{yz} & D_{zz} \end{pmatrix}$$

is a real Hermitian positive definite matrix, i.e. the matrix is symmetric with real and positive eigenvalues. The evaluation of the eigensystem of a tensor yields the major eigenvector which correlates with the direction of highest diffusion and consequently with the mean fiber direction within the voxel. Eigenvectors and respective eigenvalues serve as a basis for most DTI visualization approaches.

### 2.2 Fiber tracking

A very descriptive and popular approach for visualizing diffusion tensor data is fiber tracking. The trajectories extracted by integrating the major eigenvector field are assumed to coincide with white matter fiber bundles. Note that the term 'fibers' is used for streamlines which do not represent real anatomical fibers but provide an abstract model of neural structures. Starting from seed voxels, the tracking is performed in forward and backward direction with sub-voxel precision. For the selection of seed voxels and for aborting the streamline propagation, fractional anisotropy (FA) [13] is used as threshold:

$$FA = \sqrt{\frac{3((\lambda_1 - \langle \mathbf{D} \rangle)^2 + (\lambda_2 - \langle \mathbf{D} \rangle)^2 + (\lambda_3 - \langle \mathbf{D} \rangle)^2)}{2(\lambda_1^2 + \lambda_2^2 + \lambda_3^2)}}$$

where  $\langle \mathbf{D} \rangle$  is a measure for the mean diffusivity which characterizes the overall amount of diffusion  $\langle \mathbf{D} \rangle = \frac{1}{3} \text{Trace}(\mathbf{D}) = \frac{1}{3} \sum_i \lambda_i$ . FA represents the degree of anisotropic diffusion and therefore is considered to be a proper measure for the presence of white matter. Following this assumption, voxels with high FA are used as seed voxels. If FA drops below a certain threshold, the tracking stops.

Accordingly, a single tracking step of the streamline propagation looks as follows: The tensor at the current end point of the fiber is computed using trilinear interpolation which is separately performed for each tensor component. Subsequently, the eigensystem of the tensor is calculated providing the major eigenvector which correlates with the direction of highest diffusion. In case of Euler integration, the next streamline propagation step would be in direction of the major eigenvector. For reasons of numerical accuracy, we apply a higher order integration scheme (Runge-Kutta of order four) which needs repeated tensor interpolation and major eigenvector computations until the direction of streamline propagation is determined. The step size

is set to a fixed value which is a quarter of the voxel size. Since the field of the major eigenvectors does not correspond to a flow field we found it more convenient to choose a sufficiently low fixed step size instead of adaptive adjustments. In contrast to nerves, flows consisting of particles possess physical properties such as inertia which ensure that sudden changes of direction do not occur. For fiber tracking a fixed step size is better to prevent missing turnoffs. Apart from the FA threshold for the termination of fiber tracking, fiber propagation is aborted if a streamline has reached a maximum length. If a minimum length is not reached, the fiber is rejected. Beside these thresholds one may choose between a tracking encompassing the whole brain and a tracking extracting fibers that run through user-defined ROIs. The latter approach enables the reconstruction of separate tract systems which is of special interest for medical applications.

### 2.3 Evenly spaced streamlines

The basic principle of evenly spaced streamlines is to calculate streamlines until a user-defined density level is reached. Thereby, a regular distribution of the streamlines is achieved and areas with a sparse distribution of streamlines are filled. In the context of fiber tracking, this is a highly desirable property to capture all features, i.e. the location of white matter, of the diffusion tensor field.

The basic algorithm for evenly spaced streamlines computes an initial streamline and chooses new seed points in its vicinity with distance  $d_{seed}$ . Starting at these seed points, the new streamlines are propagated in both forward and backward direction until they come closer than  $d_{sep}$  to each other or the boundary of the volume is reached. Thereby,  $d_{seed}$  is slightly higher than  $d_{sep}$  to avoid the new streamline to terminate instantly in the first step.

In addition to standard streamline propagation, the algorithm for computing evenly spaced streamlines comprises additional processing steps, namely distance control between adjacent streamlines (Section 2.3.1) and selection of additional seed points (Section 2.3.2).

#### 2.3.1 Distance control

The density of a streamline bundle is actually a global feature. To obtain a uniform density, this

global feature has to be locally determined during streamline reconstruction. Therefore, a technique for local distance control is needed to ensure that streamlines do not come closer to each other than the separating distance  $d_{sep}$ . In order to obtain acceptable computation times for distance control, only the sample vertices of the streamline are considered for distance computations. For each propagation step, the distance check is performed to verify whether the streamline gets too close to another one. A simple check would test the new streamline vertex  $p$  against all sample vertices of all other streamlines which would be rather inefficient. This is circumvented by using a Cartesian grid with voxel size  $d_{sep}$  superimposed on the domain. Each voxel of this grid provides a list of pointers to the sample points located within this voxel. For each computed streamline vertex this data structure is updated and the new vertex is inserted. This data structure is shown in Figure 1.

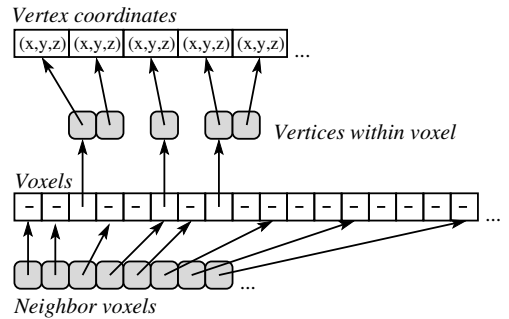


Figure 1: Data structure for fast access to neighbor vertices of a given voxel.

In order to obtain all vertices that are potentially closer than  $d_{sep}$  to  $p$ , the voxel containing  $p$  as well as all 26 surrounding neighbor voxels are determined within the Cartesian grid. The distance between  $p$  and each vertex referred to by the surrounding voxels is computed. If this distance is less than  $d_{sep}$ , streamline propagation is aborted.

To efficiently decide whether a streamline has to be aborted, the number of distance computations has to be minimized. Therefore, we optimized the order in which the surrounding voxels and the referred vertices are processed. For vertices contained within the center voxel, the probability that  $p$  is closer than  $d_{sep}$  is very high and this voxel is pro-

cessed first. The voxels sharing a face with the center voxel are processed next, followed by voxels sharing an edge. Finally, the diagonal adjacent voxels only sharing a vertex with the center voxel are examined.

Another point to mention is that the step size for streamline integration and  $d_{sep}$  are not fully independent. Since only the distance between sample vertices of the streamlines is computed and not the actual distance to the segments of another streamline,  $d_{sep}$  should not be smaller than the step size for fiber tracking. This guarantees that a vertex will not be located much closer to a fiber segment than  $d_{sep}$ . If  $d_{sep}$  equals the step size, a vertex is not closer to a fiber segment than  $\frac{\sqrt{3}}{2}d_{sep}$ , which is the worst case as shown in Figure 2.

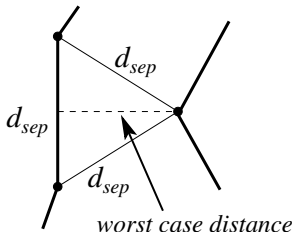


Figure 2: If  $d_{sep}$  equals the step size for streamline propagation, the worst case and minimum distance between fibers is  $\frac{\sqrt{3}}{2}d_{sep}$ .

### 2.3.2 Selection of seed points

The basic principle for seed point selection is to determine all seed points which can be found from an existing streamline before continuing with another one. Thereby, seed points at a distance  $d = d_{seed}$  from the sample vertices are used for initiating streamline propagation. A queue is used to store the streamlines and to control the order in which streamlines are processed.

The algorithm for evenly spaced streamlines was originally designed for 2D [10, 11]. For the visualization of neural pathways using streamlines this approach was extended to three dimensions. Considering seed point selection, this was accomplished as follows (Figure 3): To obtain new seed points in the vicinity of a sample vertex with adjacent streamline segments  $\vec{s}_1$  and  $\vec{s}_2$ , these segments are averaged to obtain the normal  $\vec{n}$  of the plane where the

new seed points will be placed. To obtain a vector  $\vec{v}_1$  perpendicular to  $\vec{n}$ , the component of  $\vec{n}$  which is closest to zero is set to zero, the other components are swapped and one of them is negated. The resulting vector  $\vec{v}_1$  in the plane is scaled to the length  $d_{seed}$ . Another vector  $\vec{v}_2$  in the plane perpendicular to  $\vec{v}_1$  is obtained by computing the cross product between  $\vec{n}$  and  $\vec{v}_1$ . Analogous to  $\vec{v}_1$ ,  $\vec{v}_2$  is also scaled to  $d_{seed}$ . To avoid patterns and moire effects in regular datasets, new seed positions are selected at random directions depicted by  $\vec{v}'_1$  and  $\vec{v}'_2$  ( $\alpha$  is some random angle):

$$\begin{aligned}\vec{v}'_1 &= \cos(\alpha) \vec{v}_1 + \sin(\alpha) \vec{v}_2 \\ \vec{v}'_2 &= \cos(\alpha + 90^\circ) \vec{v}_1 + \sin(\alpha + 90^\circ) \vec{v}_2\end{aligned}$$

In addition to the seed points denoted by  $\vec{v}'_1$  and  $\vec{v}'_2$ , two further seed points are obtained by negating all components of  $\vec{v}'_1$  and  $\vec{v}'_2$ , respectively. Afterwards, streamline propagation is started provided that the FA value at these seed points is high enough for tracking.

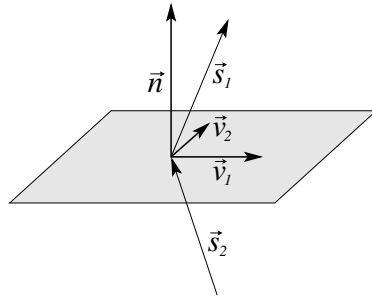


Figure 3: 3D seed point selection. The directions of adjacent segments are averaged to obtain the normal vector of the plane containing the new seed points.

### 2.4 Adaptive control of the separating distance for visual enhancement

Beside the major eigenvector indicating the direction of main diffusion, the eigenvalues of the tensor provide information about the magnitude of anisotropic diffusion. Different scalar measurements for this quantity have been presented. A commonly used metric is FA [13] which is related to the presence of oriented structures and describes a directional bias. An approach presented by Westin

et al. [12] characterizes the shape of a tensor by assigning coordinates in a barycentric space. This space is spanned by three basis tensor shapes which are linear, planar and spherical diffusion. The linear component  $c_l$  thereby reveals the information whether the largest eigenvalue of a tensor dominates, which corresponds to strong anisotropic diffusion.

For each tensor, these scalar metrics provide further information about diffusion characteristics. To incorporate this additional information into a more comprehensive streamline visualization, an alternative distance scheme was developed. An adaptive density control was implemented to obtain fibers of higher density in areas of high anisotropic diffusion as indicated by the diffusion metrics. Thereby, thick and dominant fiber structures with a high anisotropic diffusion are visualized with denser streamlines. Consequently, major fiber bundles become visually much more apparent.

The scalar measure of FA as well as the barycentric coordinates are in the range of 0 and 1. The values  $d_{sep-a}$  and  $d_{seed-a}$  for adaptive density control are obtained by multiplying the initial distance control values  $d_{sep}$  and  $d_{seed}$  with the distance control value obtained from the metric. Since a high FA or  $c_l$  value indicate anisotropic diffusion,  $(1 - FA)$  or  $(1 - c_l)$  are used as distance weights. In addition to that, a lower bound for  $d_{sep-a}$  and  $d_{seed-a}$  has to be specified to prevent  $d_{sep-a}$  and  $d_{seed-a}$  from dropping below the step size for streamline propagation. The maximum value of  $d_{sep-a}$  equals  $d_{sep}$ , the maximum value of  $d_{seed-a}$  equals  $d_{seed}$ .

From an implementation point of view, this adaptation is easily combined with the original approach. Since the distance measure varies between the tracking step size (minimum value) and  $d_{sep}$  (maximum value), the superimposed grid remains the same. However, for regions of high density, the grid is coarser than actually required which leads to a higher number of distance checks than necessary.

## 2.5 Region-of-interest-based tracking using evenly spaced streamlines

ROIs are an essential technique to obtain separate tract systems for analyzing and separating white matter anatomy within the human brain. Based on FA maps or anatomical landmarks, ROIs are defined which either serve as seed regions for the track-

ing [2] or are used to distinguish and display the relevant streamlines during visualization [6, 14]. In case of multiple ROIs, only fibers crossing all ROIs are maintained.

However, the approach for evenly spaced streamlines is originally not adequate for the combination with ROI tracking because of the following reasons: First of all, the approach for evenly spaced streamlines may cause streamlines running through the ROI to terminate early if they get too close to each other. Additionally, shorter streamlines filling gaps between the streamlines running through the ROIs are not maintained since they do not cross the ROIs.

To integrate evenly spaced streamlines into standard fiber tracking, we pursued the following approach: The density threshold  $d_{sep}$  introduced in the context of evenly spaced streamlines is used as additional criterion for aborting fiber propagation. This initial set of fibers serves as a basis for the generation of evenly spaced streamlines filling sparse regions. In a first iteration, initial streamlines are generated and seed points with distance  $d_{seed}$  to the sample vertices are determined as described in Section 2.3.2. Then, the first generation of evenly spaced streamlines is computed based on these seed vertices. A second generation of evenly spaced streamlines may be computed based on the first generation, and so on. This iterative process enables to fill areas of white matter between the initial streamlines. However, the number of generations of evenly spaced streamlines should be low to avoid expansion to undesired areas.

## 3 Results and Discussion

The approach for evenly spaced streamlines including adaptive step size and ROI based tracking was tested with 2 DTI datasets of healthy volunteers. All computations were performed on a PC equipped with an AMD Athlon (1.2 GHz). A number of setups were considered and compared:

**Tracking of the whole brain with and without evenly spaced streamlines:** In Figure 4 a standard fiber tracking of the whole brain (*left*) in comparison to fiber tracking using evenly spaced streamlines (*middle, right*) is shown. Figure 4 clearly shows that standard fiber tracking produces regions of sparse fiber density as well as cramped ar-

eas. Contrarily, fiber tracking incorporating evenly spaced streamlines provides a constant fiber density and therefore an unbiased representation of the data.

The computation time for standard tracking (*left*) amounted to 8 sec. In case of evenly spaced streamlines, the computation time for a spacing of  $d_{sep} = 0.5$  mm (*middle*) was 134 sec. For a spacing of  $d_{sep} = 1.5$  mm (*right*) the computation time amounted to 23 sec.

### Tracking of the whole brain, evenly spaced streamlines with and without adaptive distance control:

Contrary to Figure 4 where a constant spacing was used between streamlines, in Figure 5 the density of streamlines was adaptively adjusted according to the local FA value. Similarly to standard flow visualization where dense streamlines indicate that velocities and pressure gradients are high, the approach for adaptive spacing ensures that major tract systems with a high anisotropic diffusion are represented with dense streamlines. The pyramidal tract denoted in blue as well as the fiber bundles of the corpus callosum in red can be clearly identified.

In each image, the density  $d_{sep-a}$  varies between 0.5 mm which is the step size for tracking and 2 mm (*left*), 3 mm (*middle*) and 5 mm (*right*). Computation times were 142 sec, 98 sec and 58 sec, respectively.

### ROI tracking with and without evenly spaced streamlines:

Figure 6 shows a ROI tracking of the pyramidal tract. In a first step, an initial ROI tracking taking into account  $d_{sep}$  for streamline termination is computed (*left*). In a second pass, the first generation of evenly spaced streamlines is generated (*middle*). Based on the initial tract, sparse regions are filled with streamlines. A third pass (*right*) based on the initial streamlines and the first generation of evenly spaced streamlines further fills the volume. With this technique, the concept of evenly spaced streamlines was adapted to ROI tracking providing dense tracts capturing the features within the data.

## 4 Conclusion and Future Work

The concept of evenly spaced streamlines was adapted to streamline visualization of DTI data. An adaptive distance control was added to obtain

a varying density of fibers depending on the local anisotropic diffusion characteristic. Dominant tract systems become much more apparent with this technique. Additionally, approaches for incorporating evenly spaced streamlines into ROI tracking were presented. Overall, evenly spaced streamlines proved to be an adequate technique for comprehensive streamline-based visualization of DTI data.

Future work will consider and vary the parameters to produce streamline visualizations of DTI data ranging from hand-drawing style to LIC-like [15] style.

## 5 Acknowledgments

This work was supported by the Deutsche Forschungsgemeinschaft in the context of SFB 603, Project C9 and the Graduate Research Center “3D Image Analysis and Synthesis”.

We would like to thank Helwig Hauser, VRVis Research Center (VRVis), Vienna, Austria, for interesting discussions and valuable suggestions on the topic of streamline visualization.

## References

- [1] M. Björnemo, A. Brun, R. Kikinis, and C.-F. Westin, “Regularized Stochastic White Matter Tractography Using Diffusion Tensor MRI,” in *Proc. MICCAI*, pp. 435–442, 2002.
- [2] L. Zhukov and A. Barr, “Oriented Tensor Reconstruction: Tracing Neural Pathways from Diffusion Tensor MRI,” in *Proc. IEEE Visualization*, 2002.
- [3] S. Mori, B. Crain, V. Chacko, and P. van Zijl, “Three-dimensional tracking of axonal projections in the brain by magnetic resonance imaging,” *Ann Neurol* **45**, pp. 265–269, February 1999.
- [4] P. Basser, S. Pajevic, C. Pierpaoli, J. Duda, and A. Aldroubi, “In Vivo Fiber Tractography Using DT-MRI Data,” *Magn. Res. Med.* **44**, pp. 625–632, 2000.
- [5] S. Mori and P. van Zijl, “Fiber tracking: principles and strategies – a technical review,” *NMR Biomed* **15**, pp. 468–480, 2002.
- [6] P. Fillard, J. Gilmore, W. Lin, and G. Gerig, “Quantitative analysis of white matter fiber properties along geodesic paths,” in *Proc. MICCAI*, 2003.

- [7] A. Vilanova, G. Berenschot, and C. van Pul, "Dti visualization with streamsurfaces and evenly-spaced volume seeding," in *Proc. Joint EG/IEEE TCVG VisSym*, pp. 173–182, 2004.
- [8] C. Clark, T. Barrick, M. Murphy, and B. Bell, "White matter fiber tracking in patients with space-occupying lesions of the brain: a new technique for neurosurgical planning?," *Neuroimage* **20**(3), pp. 1601–1608, 2003.
- [9] C. Nimsky, O. Ganslandt, P. Hastreiter, R. Wang, T. Benner, A. Sorensen, and R. Fahlbusch, "Preoperative and Intraoperative Diffusion Tensor Imaging-based Fiber Tracking in Glioma Surgery," *Neurosurgery* **56**(1), pp. 130–138, 2005.
- [10] B. Jobard and W. Lefer, "Creating evenly-spaced streamlines of arbitrary density," in *Visualization in Scientific Computing, Proc. of the 8. Eurographics Workshop*, pp. 43–56, 1997.
- [11] G. Turk and D. Banks, "Image-guided streamline placement," in *Proc. SIGGRAPH*, pp. 453–460, ACM Press, 1996.
- [12] C. Westin, S. Maier, H. Mamata, A. Nabavi, F. Jolesz, and R. Kikinis, "Processing and visualization for diffusion tensor MRI," *Med Image Anal* **6**(2), pp. 93–108, 2002.
- [13] P. Basser and C. Pierpaoli, "Microstructural and physiological features of tissues elucidated by quantitative-diffusion-tensor MRI," *J Magn Reson B* **111**(3), pp. 209–219, 1996.
- [14] D. Akers, A. Sherbondy, R. Mackenzie, R. Dougherty, and B. Wandell, "Exploration of the brain's white matter pathways with dynamic queries," in *Proc. IEEE Visualization*, pp. 377–384, 2004.
- [15] B. Cabral and L. Leedom, "Imaging vector fields using line integral convolution," in *Proc. SIGGRAPH*, pp. 263–270, ACM Press, 1993.

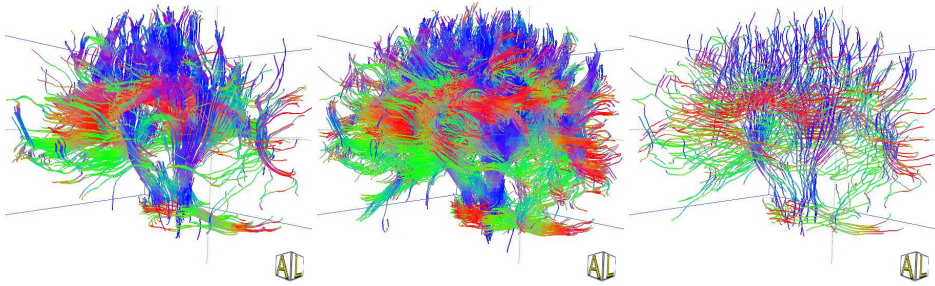


Figure 4: Comparison of standard fiber tracking (*left*) and tracking based on evenly spaced streamlines with density  $d_{sep} = 0.5$  mm (*middle*) and  $d_{sep} = 1.5$  mm (*right*).

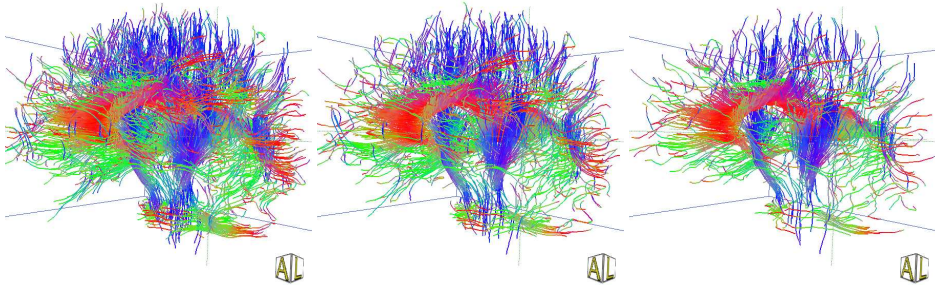


Figure 5: Adaptive distance control for tracking using evenly spaced streamlines emphasizes dominant tract systems with dense streamlines. The spacing  $d_{sep-a}$  between adjacent streamlines is adjusted depending on the local FA and varies between 0.5 mm and 2 mm (*left*), 3 mm (*middle*) and 5 mm (*right*).

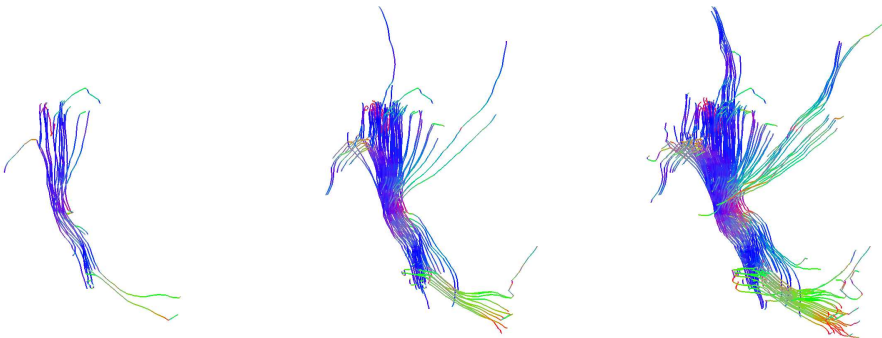


Figure 6: ROI tracking of the pyramidal tract (*left*), first (*middle*) and second (*right*) generation of evenly spaced streamlines. Incorporation of evenly spaced streamlines into ROI tracking provides dense tracts.